53. Sterically Congested Phosphite Ligands: Synthesis, Crystallographic Characterization, and Observation of Unprecedented Eight-Bond $^{31}P,^{31}P$ Coupling in the ^{31}P-NMR Spectra

by **Stephen D. Pastor**[a])*, **Sai P. Shum**[a]), **Ronald K. Rodebaugh**[b]), and **Anthony D. Debellis**[c])

[a]) Synthetic Research Department, [b]) Analytical Research Department, and [c]) Scientific Computing Department, Additives Division, *Ciba-Geigy Corporation*, Ardsley, New York 10502, USA

and **Frank H. Clarke**

Therapeutic Area Support, Pharmaceutical Division, *Ciba-Geigy Corporation*, Summit, New Jersey 07901, USA

(3.VIII.92)

The synthesis and characterization of 2-{1-{3,5-bis(1,1-dimethylethyl)-2-{[2,4,8,10-tetrakis(1,1-dimethylethyl)dibenzo[*d,f*][1,3,2]dioxaphosphepin-6-yl]oxy}phenyl}ethyl}-4,6-bis(1,1-dimethylethyl)phenyl diphenyl phosphite (**6**) is described. In the ^{31}P-NMR spectrum (^1H-decoupled) of **6**, an unprecedented eight-bond P,P coupling of $J = 72.8$ Hz is observed. In the X-ray crystal structure of **6**, an intramolecular P–P distance of 3.67 Å is found, which is within the sum of the *van-der-Waals* radii of the P-atoms. The observed intramolecular P–P distance suggests that a through-space coupling mechanism is operative. The solid-state conformation of **6** is compared to the conformation obtained by semi-empirical MO geometry optimizations (PM3 method). The calculated geometry suggests that the solid-state structure is near a true energy minimum, but that crystal-packing forces decrease the intramolecular P–P distance in the solid state. In the absence of crystal-packing forces, however, the collisional and vibrational energy available in solution may lead to the population of states with a shortened intramolecular P–P distance in **6**. The proximity of the P-atoms in **6** is due to restricted conformational freedom resulting from steric congestion within the molecule. The free energy of activation ($\Delta G^* = 10.2$ and 10.8 kcal/mol for unequal populations of exchanging conformers) for ring inversion of the dibenzo[*d,f*][1,3,2]dioxaphosphepin ring in **6** is determined by variable-temperature ^{31}P-NMR spectroscopy. Semi-empirical MO calculation on model compounds suggest that the structure of the transition state for ring inversion has the two aryl rings and O-atoms in a common plane, with the P-atom lying above this plane.

Introduction. – The development of P-ligands for transition-metal-catalyzed reactions has evolved at a prodigious rate during the last two decades. Sterically hindered ligands were designed to provide unique coordination spheres for transition metals [1]. Recently, we reported a class of sterically congested molecules with unusual spectral properties [2]. In particular, an unprecedented seven- and eight-bond P,P coupling of $^7J(P(1),P(2)) = 30.3$ Hz and $^8J(P(1),P(2)) = 30.6$ Hz was observed in the solution ^{31}P-NMR spectra (^1H-decoupled) of **1** and **2**, respectively.

The observation of $^8J(P(1),P(2)) = 30.6$ Hz in the ^{31}P-NMR spectrum of **2** in which the aromatic π systems are separated by a sp^3-hybridized C-atom suggests that a through-space coupling mechanism is operative. The intramolecular P–P distance of **1** in the solid state (3.70 Å) is within the sum of the *van-der-Waals* radii of the P-atoms (3.80 Å), whereas the intramolecular P–P distance of **2** (4.50 Å) is greater than the sum of the *van-der-Waals* radii. The collisional and vibrational energy of **1** and **2** in solution may, however, lead to the population of states with shortened intramolecular P–P distances [3].

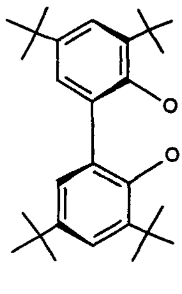

1

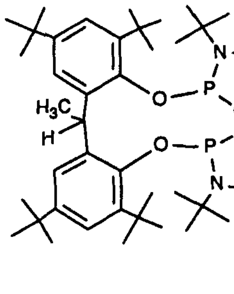

2

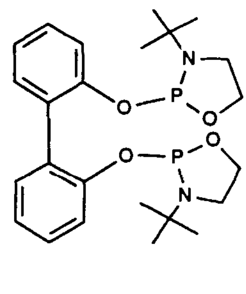

3

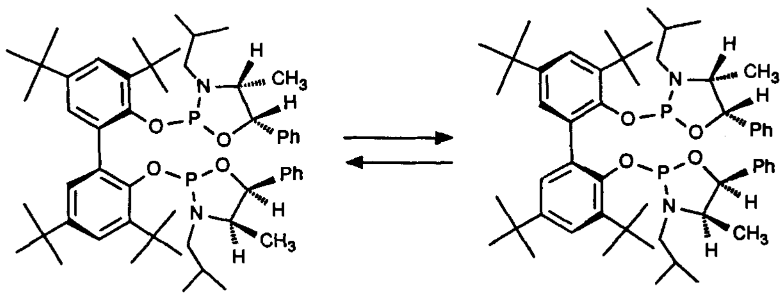

4 **5**

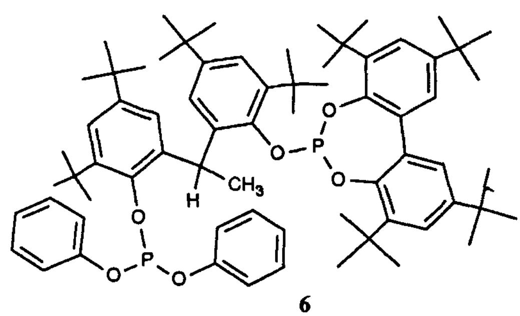

6

The loss of observable P,P coupling in **3** and other model compounds [2] support the contention that the proximity of the P-atoms in **1** and **2** is due to restricted conformational freedom resulting from steric congestion within these molecules.

The observation of nonequivalent P-atoms in the ^{31}P-NMR spectrum of **1** requires that rotation about the C–C bond connecting the two aryl groups is slow on the NMR time scale, which is consistent with the observed ($P(1)R^*$, $P(2)S^*$, R^*_{axial})-configuration in the solid state. This must be the case, because rapid rotation about this single bond (a chiral axis) would render the P-atoms enantiotopic and, therefore, equivalent in the ^{31}P-NMR spectrum. Further evidence for restricted rotation in these molecules comes from both the isolation and the observed equilibration of enantiomerically pure **4** and **5**, which differ only in the absolute configuration of the chiral axis [4]. We described [4] [5] both the characterization of a Pt^{II} complex of **1** and transition-metal-catalyzed asymmetric hydrogenations and hydrosilations using **4** as a chiral ligand.

In an extension of this work, we report herein the detailed synthesis and crystallographic characterization of the sterically congested phosphite **6**, which is claimed as a ligand for transition-metal-catalyzed hydroformylations [6]. The phosphite ligand **6** and its analogs are of particular interest, because they contain both chiral center and a chiral axis, and, in this regard, are potential model ligands useful to explore the notion of chiral cooperativity [7].

Results and Discussion. – *Synthesis*. The reaction of bis(phenol) **7** [8] with excess PCl_3 in toluene catalyzed by 1-methylpyrrolidin-2-one gave phosphorochloridite **8** (*Scheme*). In the ^{31}P-NMR spectrum of **8**, a resonance is observed at δ 173.3, which is in the region expected for a phosphorochloridite [9][1]). Phosphite **10** was prepared by the reaction of **8**

Scheme

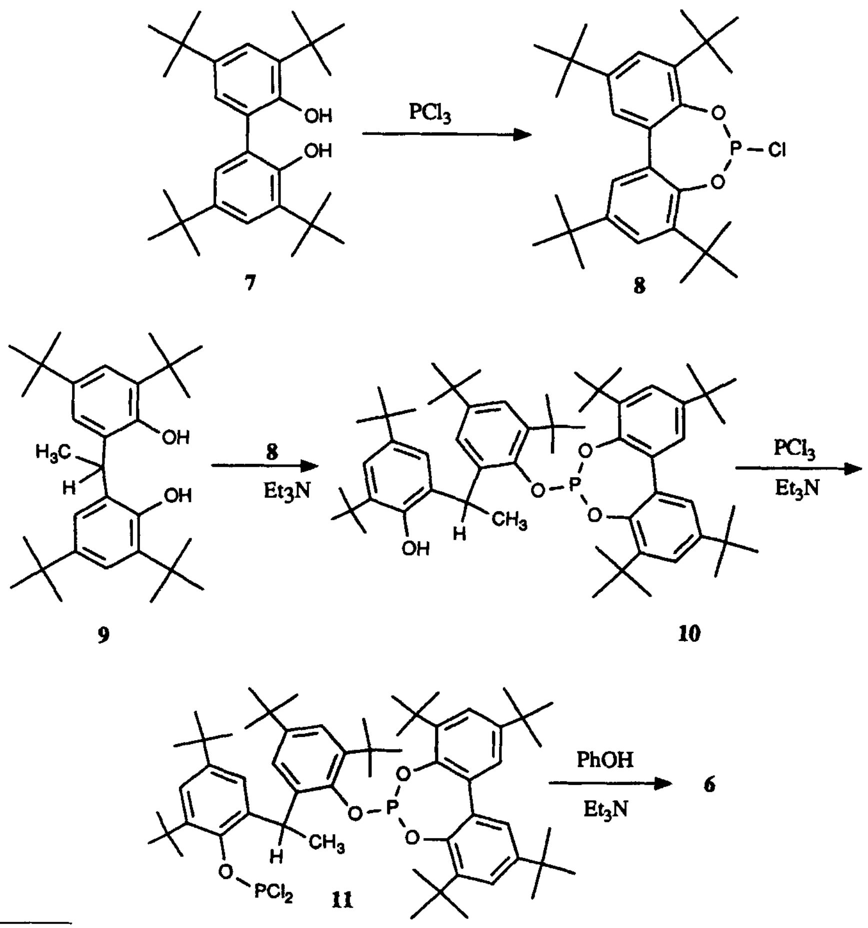

[1]) For monographs on ^{31}P-NMR spectroscopy, see [9].

with 1 equiv. of ethylidenebis(phenol) **9** (74% yield, after recrystallization) [10] [11][2]), and phosphorodichloridite **11** was obtained from **10** and 1 equiv. of PCl_3. Surprisingly, in the ^{31}P-NMR spectrum of **11**, an eight-bond P,P coupling of $J = 136$ Hz is observed (*vide infra*). Finally, the reaction of **11** with 2 equiv. of phenol in the presence of a base gave bis(phosphite) **6** (32% yield, after recrystallization).

NMR Spectral Data. In the ^{31}P-NMR spectrum (^{1}H-decoupled) of the dichloridite **11**, four lines are observed with relative intensities and splittings consistent with an *AB* system (pseudo-*q*). An obvious alternative is that the four resonances arise from a mixture of diastereoisomers because of the presence of both a chiral center and a chiral axis in **11**. The 2D homonuclear ^{31}P-COSY-NMR spectrum of **11** confirms the existence of coupling between the two P-atoms. Unfortunately, suitable crystals for X-ray crystallographic analysis could not be grown.

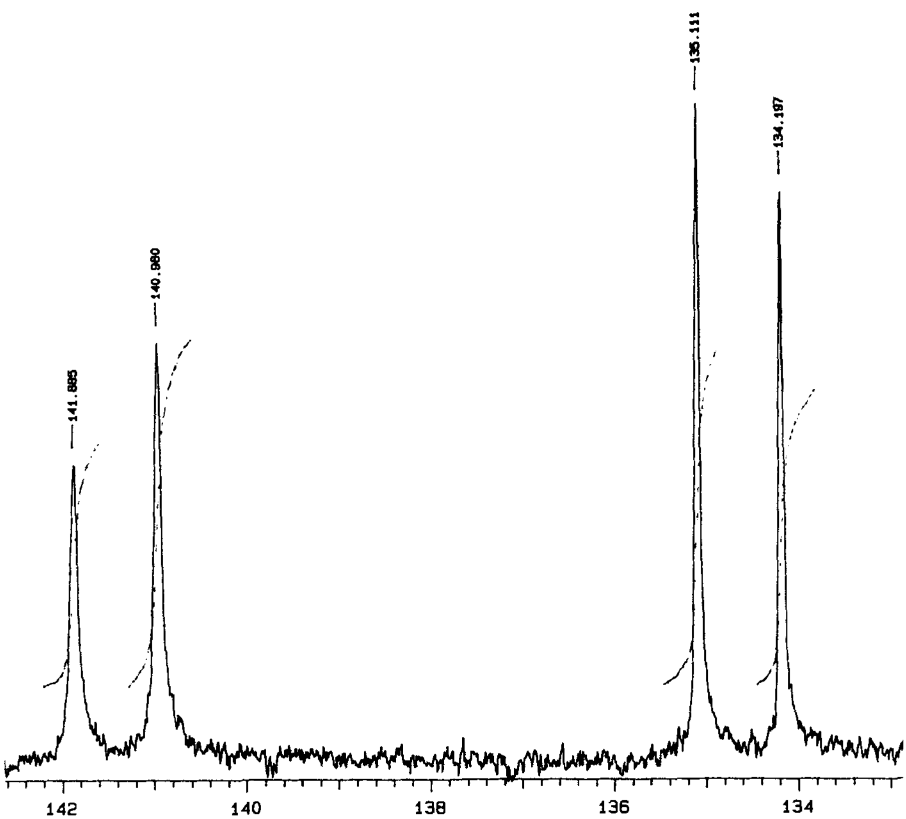

Fig. 1. ^{31}*P-NMR Spectrum* (^{1}H-decoupled) *of* **6**

In the ^{31}P-NMR spectrum of bis(phosphite) **6**, an eight-bond P,P coupling of $J = 72.8$ Hz is observed (*Fig. 1*). The existence of coupling between the two P-atoms of **6** is demonstrated both by a 2D homonuclear ^{31}P-COSY-NMR experiment (*Fig. 2*) and by obtaining the ^{31}P-NMR spectrum at two different field strengths. The downfield '*d*' at δ 141.8 is assigned to the P-atom in the dibenzo[*d,f*][1,3,2]dioxaphosphepin moiety based upon both the $\delta(^{31}P)$'s previously reported for this ring system [10–12] and the $\delta(^{31}P)$ of the dioxaphosphepin P-atom observed for **10** and **11**.

[2]) For a closely related methodology, see [11].

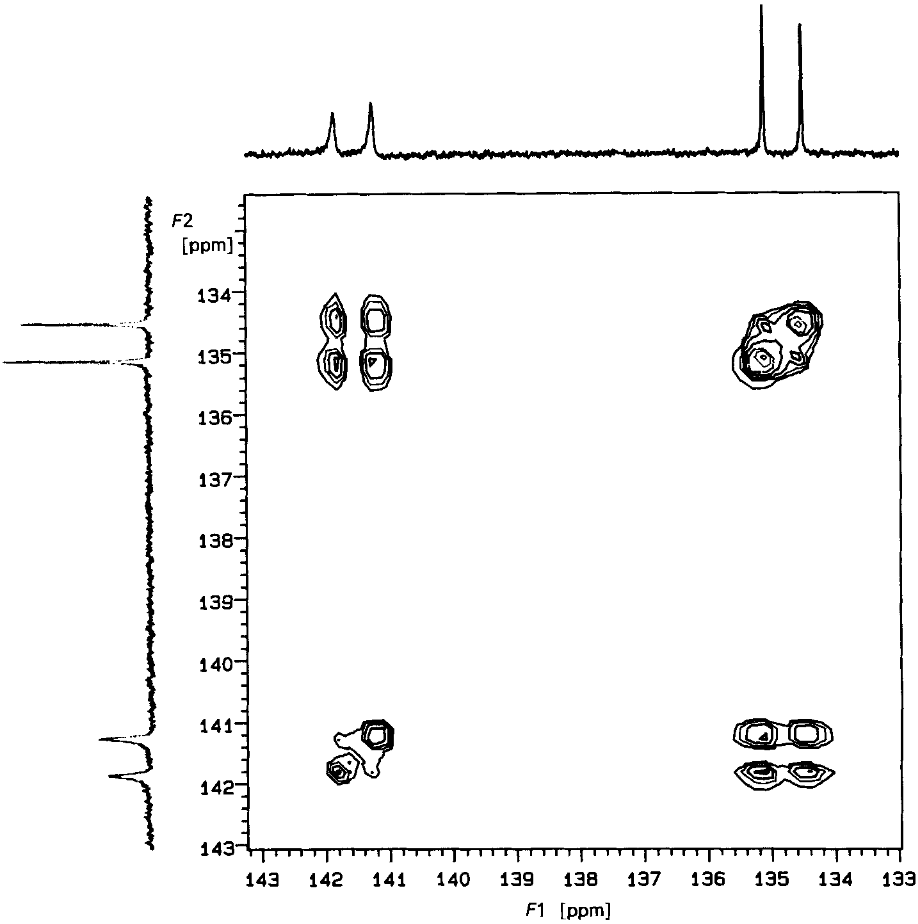

Fig. 2. *2D Homonuclear ^{31}P-COSY-NMR of* **6**

In the ^{13}C-NMR spectrum of **6**, the C(15) methine atom[3]) of the ethylidene bridge is coupled to both P-atoms (^4J(C,P) = 11.4 and ^4J(C,P) = 26.9 Hz). That the observed splitting is due to a ^4J(P,C) is confirmed by obtaining the ^{13}C-NMR spectrum at two different field strengths. Furthermore, a five-bond ^5J(H,P) = 20.5 Hz for C*H*(15) is observed in the 500-MHz ^1H-NMR spectrum of **6**. In the ^1H-NMR spectrum of **6**, 8 resonances integrating to 9 H each are observed that are assigned to the 8 nonequivalent *t*-Bu groups. The ^{13}C- and ^1H-NMR spectra of **6** are fully consistent with the structure illustrated.

X-Ray Crystal Structure. Upon growing suitable crystals, the X-ray crystal structure of **6** was obtained (*Fig. 3*, *Table 1*). In the solid state, an intramolecular P–P distance of 3.67 Å is found that is within the sum of their *van-der-Waals* radii (*Fig. 4*). Although caution must be observed in extrapolating from the solid-state to solution conformation, because the lattice energy and the resultant crystal-packing effects can render the confor-

[3]) The atom numbers refer to the numbering system used for the X-ray crystal structure of **6**, see *Figs. 3* and *4*.

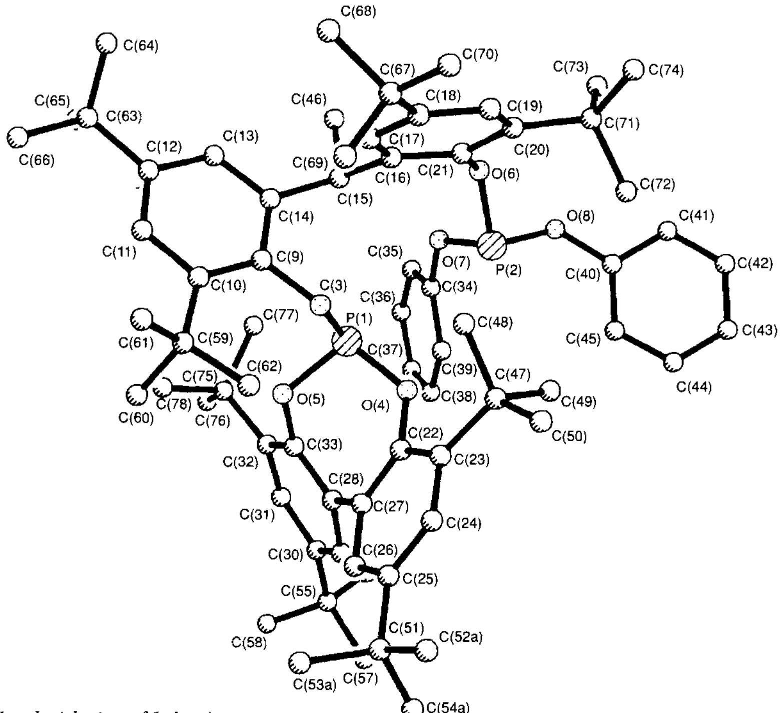

Fig. 3. *Ball and stick view of* **6** *showing the crystallographic numbering scheme* (arbitrary)

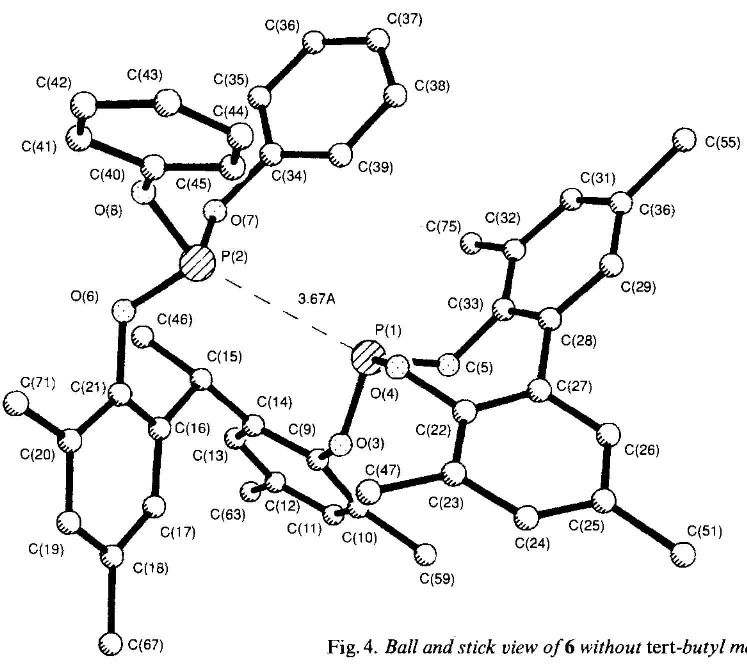

Fig. 4. *Ball and stick view of* **6** *without* tert-*butyl methyl groups*

Table 1. *Crystal and Data Collection Parameter for* **6**

Crystal Data:		*Data Collection:*	
Formula	$C_{70}H_{85}O_6P_2$	Temp.	296 K
Formula weight [$g \cdot mol^{-1}$]	1084.3	Diffractometer type	*Siemens R3m/V*
Color	colorless prism	Radiation	CuK_α (λ = 1.54178 Å)
Crystal system	triclinic	Monochromator	orientated graphite crystal
Space group	$P\bar{1}$	2θ Range	3.15–115.0°
Z	2	Scan type	2Θ-Θ
Cell parameters	a = 14.7230 (10) Å	Scan range (w)	0.50° plus $K\alpha$ separation
	b = 14.8710 (10) Å	Scan speed	variable 3.00–14.65° in w
	c = 15.569 (2) Å	Standard reflections	3 measured every 100 reflections
	α = 80.810 (10)°	Index ranges	$-16 \leqslant h \leqslant 9$; $-16 \leqslant k \leqslant 16$;
	β = 85.100 (10)°		$0 \leqslant l \leqslant 16$
	γ = 89.820 (10)°	Reflections collected	8114
Volume	V = 3352.6 (6) $Å^3$	No. of observed reflections ($F > 4.0\sigma(F)$)	7847
d_{calc}	1.074		
Absorption coefficient	0.934 mm^{-1}		
Crystal size	0.1 × 0.4 × 0.6 mm	Independent reflections	7848 (R_{int} = 1.34%)
$F(000)$	1166		

Solution and Refinement:	
System used	*Siemens* SHELXTL PLUS (VMS)
Solution	direct methods
Refinement method	full-matrix least-squares
Quantity minimized	$\Sigma w(F_o - F_c)$
H-Atoms	riding model; fixed isotropic U
Weighing scheme	$w^{-1} = \sigma^2(F) + 0.0050F^2$
Number of parameters refined	730
R (obs.)	0.0756
R_w (obs.)	0.1158
R (all data)	0.0884
R_w (all data)	0.1165
Goodness-of-fit	1.31
Largest and mean Δ/σ	0.086; 0.011
Data-to-parameter ratio	10.7:1
Largest difference peak	0.55 $eÅ^{-3}$
Largest difference hole	−0.38 $eÅ^{-3}$

mations different (*vide infra*), the observed intramolecular P–P distance suggest that a through-space coupling mechanism is operative [13][4]). The orientation of the O-atoms in the solid-state conformation of **6** further suggests that the lone-pair of electrons on the O-atoms are not involved in the transmission of coupling information.

In an effort to gain some insight on the factors responsible for the solid-state conformation of **6**, semi-empirical MO geometry optimizations were performed starting from the geometry of the observed X-ray crystal structure. The PM3 method was chosen because of its improved handling of hypervalent compounds and the sharp potential

[4]) For leading references on the through-space coupling mechanism, see [13a]; for an example of through-space F,F coupling through an intervening phenyl group, see [13e]; for nine-bond P,P coupling mediated by π-electron contributions, see [13f]; for the geometric dependence of P,P coupling upon the orientation of the lone-pair of electrons on the P-atom, see [13g].

Table 2. *Selected Crystallographic and Calculated*[a]) *Parameters for* **6**

	Selected bond angles [°]			Selected torsion angles [°]	
	Crystallographic	Calculated		Crystallographic	Calculated
O(3)–P(1)–O(4)	101.0 (1)	99.4	C(22)–O(4)–P(1)–O(5)	–30.2	–21.7
O(3)–P(1)–O(5)	95.4 (1)	96.4	O(4)–P(1)–O(5)–C(33)	–59.9	–61.4
O(4)–P(1)–O(5)	102.3 (1)	103.4	P(1)–O(5)–C(33)–C(28)	78.7	+70.3
O(6)–P(2)–O(7)	94.4 (1)	98.2	O(5)–C(33)–C(28)–C(27)	–0.1	+6.3
O(6)–P(2)–O(8)	97.7 (1)	95.0	C(33)–C(28)–C(27)–C(22)	–51.7	–52.0
O(7)–P(2)–O(8)	95.4 (1)	100.6	C(28)–C(27)–C(22)–O(4)	4.4	–1.0
			C(27)–C(22)–O(4)–P(1)	60.7	+55.9

	Selected bond distances [Å]	
	Crystallographic	Calculated
O(3)–P(1)	1.627 (3)	1.74
O(4)–P(1)	1.612 (2)	1.71
O(5)–P(1)	1.644 (2)	1.73
O(5)–C(33)	1.401 (4)	1.36
O(4)–C(22)	1.405 (4)	1.36
C(22)–C(27)	1.382 (4)	1.41
C(33)–C(28)	1.384 (5)	1.41
C(27)–C(28)	1.506 (5)	1.48
O(6)–P(2)	1.613 (2)	1.75
O(22)–P(2)	1.644 (3)	1.71
O(4)–P(2)	1.634 (3)	1.74
O(22)–C(21)	1.400 (4)	1.37

[a]) Semi-empirical MO geometry optimization by PM3 method.
[b]) Calculated for the enantiomeric structure.

barrier at 3.0 Å observed for the AM1 P-atom [14]. The calculated gas-phase geometry of the dibenzo[*d,f*][1,3,2]dioxaphosphepin ring in **6** is nearly identical to that found in the solid state (*Table 2*). A notable exception is the systematic overestimation of the P–O bond length by *ca.* 0.1 Å. The calculated and observed absolute value of the C(22)–C(27)–C(28)–C(33) torsion angle about the single bond joining the two phenyl rings is 51.7 and 52.0°, respectively. The calculated P–P distance increases to 4.60 Å by a rotation about the C(14)–C(15) single bond with a concurrent change in bond angles about P(2). Caution must be exercised in comparing calculated and observed P–P distances, because it is generally accepted that bond angles calculated by MO calculations are accurate to within only 5°. Small errors in calculated bond angles can lead to a large error in the P–P distance, because the atoms are eight bonds apart. The calculated (104°) and observed (67°) C(9)–C(14)–C(15)–C(16) torsion angles, however, appear well outside the expected error. A reasonable explanation for this observation is that rotation about this single bond results in a reduction of steric interactions. This motion rotates the Me group of the ethylidene bridge out of the plane of the phenyl ring such that the methine proton eclipses the ring. Previous studies showed that the observed minimum-energy arrangement of analogous conformations of *o,o'*-disubstituted toluene derivatives have the methine proton eclipsing the phenyl ring [15] [16]. In addition, molecular-mechanics calculations on phenylcyclohexane produced the same result [17]. The calculated geometry suggests that the solid-state structure is near a true energy minimum, but that crystal-packing forces decrease the intramolecular P–P distance in the solid state. Never-

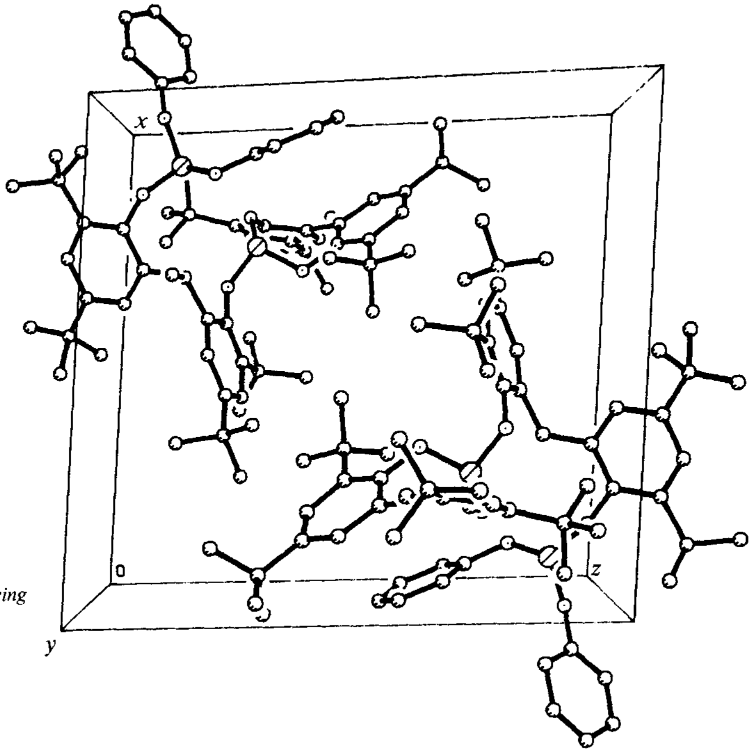

Fig. 5. *Projection along the crystallographic,* y *axis showing the crystal packing of* **6**

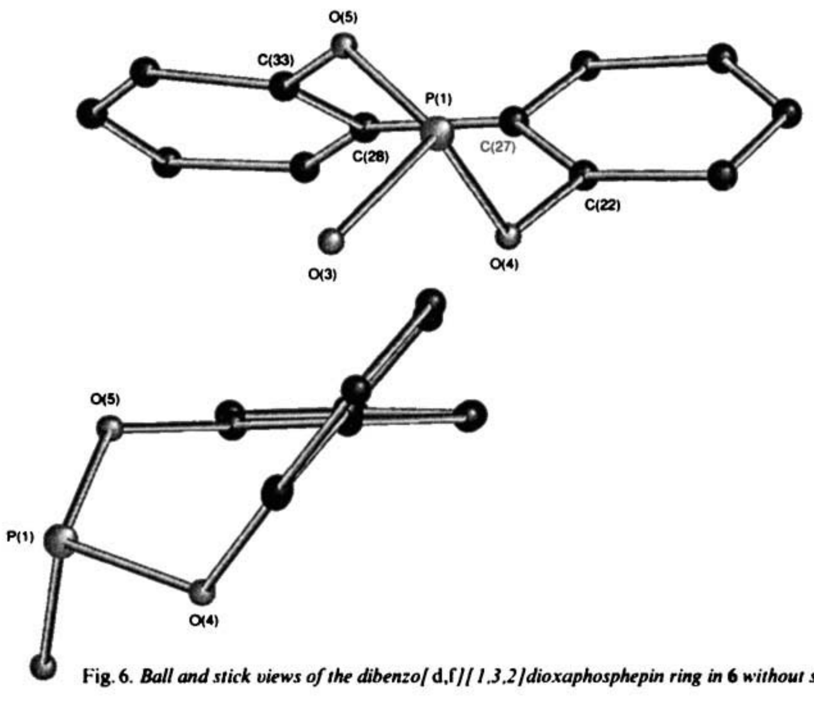

Fig. 6. *Ball and stick views of the dibenzo[*d,f*][1,3,2]dioxaphosphepin ring in* **6** *without substituents*

theless, the collisional and vibrational energy available to **6** in solution may lead to the population of states with a shortened P–P distance.

In the X-ray crystal structure of **6**, two molecules are observed in the unit cell that are related by a center of inversion (*Figs. 5* and *6*). Further, the two molecules are a pair of enantiomers. A single diastereoisomer is observed with configuration (CR^*, S^*_{axial}) in the solid state (*Fig. 7*). In solution, rapid inversion of the dibenzo[*d,f*][1,3,2]dioxaphosphepin ring (rapid 'flipping' of the two phenyl rings about the chiral axis) removes the asymmetry due to the ring, which results in an enantiomeric mixture (*vide infra*). This is the case because rapid ring inversion renders the ring achiral by rapid passage through an effectively planar transition state (or intermediate).

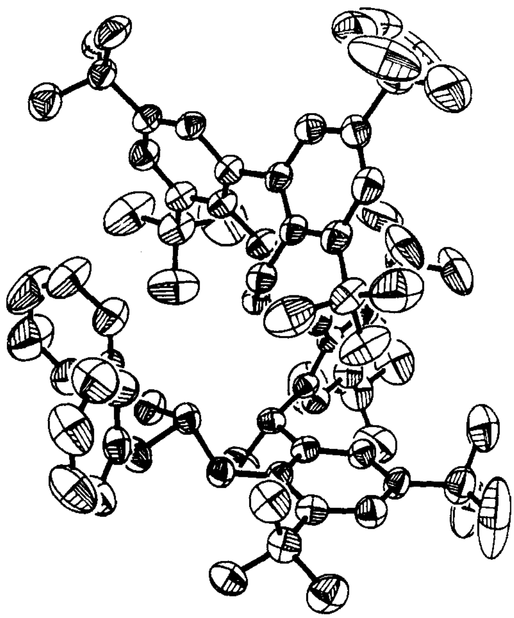

Fig. 7. *Molecular structure of* **6** *showing thermal ellipsoids*

Little information is available about the conformation of the dibenzo[*d,f*][1,3,2]dioxaphosphepin ring system in either the solid state or solution [18–20]. Quite recently, *Holmes* and coworkers reported the X-ray crystal structure for the dibenzo[*d,f*][1,3,2]dioxaphosphepin **12** [21]. They found important differences in the axial-equatorial placement (at the trigonal bipyramid) of dibenzo[*d,f*][1,3,2]dioxaphosphepins and the related dibenzo[*d,g*][1,3,2]dioxaphosphocins incorporated in pentaoxyphosphoranes with and without *t*-Bu substitution that may, at least in part, be due to a steric effect [12] [21] [22].

Previous workers suggested a twisted ring conformation for the dibenzo[*d,f*][1,3,2]dioxaphosphepin ring system, which is observed in the solid state for both **6** and **12**. Although differences may be expected because of the S-substituent in **12**, a comparison

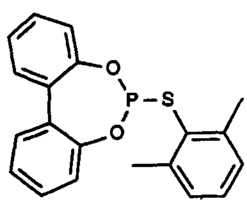

12

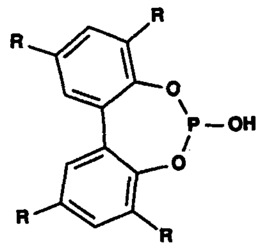

13a R = H
R = *t*-Bu

of their solid-state conformations proves interesting. The absolute value of the C(22)–C(27)–C(28)–C(33) torsion angle about the single bond joining the two phenyl rings is 51.7° in **6** compared to a smaller torsion angle of 39.6° in **12**. A O(4)–P(1)–O(5) bond angle of 102.3(1)° is found in **6**, which is similar to that in **12**. Admitting that pyramidal geometry about the P-atom is achieved when the sum of the requisite bond angles is 270°, the dioxaphosphepin P-atoms in **6** (298.7°) and **12** (298.4°) approach pyramidal geometry. The exocyclic P(2) atom in **6** is nearer to pyramidal geometry (287.5°) than the endocyclic P(1) atom.

Neglecting any electronic or steric effect due to the S-atom upon ring geometry in **12**, the larger C(22)–C(27)–C(28)–C(33) torsion angle found in **6** may be due to the larger steric interactions within the molecule. The contention that the S-atom has a negligible effect on ring geometry in **12** is supported by the fact that similar geometries about the P-atoms are found in both **6** and **12**. Further support for a steric argument is provided by the semi-empirical MO geometry optimization of the unsubstituted and *t*-Bu-substituted hypothetical model compounds **13a** and **13b**, respectively. The corresponding torsion angles calculated for **13a** (43.9°) and **13b** (53.2°) compare favorably with those observed for **12** (39.6°) and **6** (51.7°). Very recently, the corresponding torsion angles observed in the crystal structure of a molecule containing two unsubstituted dioxaphosphepin rings with three O-atoms bonded to the P-atom were −41.4° and −42.2° [23].

The intriguing question remains as to whether ring inversion of the dibenzo[*d,f*][1,3,2]dioxaphosphepin ring is rapid in solution. Slow ring inversion on the NMR time scale would be expected to lead to the observed nonequivalence of the *t*-Bu groups (*vide supra*). However, the observation of distinct resonances in both the ^{13}C- and ^{1}H-NMR spectra for each *t*-Bu group in **6** is *not necessarily* evidence for slow ring inversion. This is the case because the molecular asymmetry due to the chiral C(15) center renders each pair of *t*-Bu groups on the dibenzo[*d,f*][1,3,2]dioxaphosphepin ring diastereotopic [24][5]). The C(15) atom in **6** is both stereogenic and chirotopic. The explanation that the *t*-Bu groups are inherently nonequivalent because of the chiral center in **6** rather than because of slow ring inversion is strongly supported by the fact that the C-atoms and protons of the two PhO groups bonded to P(2) are nonequivalent in the ^{13}C- and ^{1}H-NMR spectra, respectively. This nonequivalence of the PhO groups must be due to asymmetry within the molecule.

5) For a discussion on topicity and NMR spectra, see [24].

The contention that the dibenzo[*d,f*][1,3,2]dioxaphosphepin ring of **6** is undergoing rapid ring inversion in solution on the NMR time scale was fully resolved by variable-temperature ^{31}P-NMR spectroscopy. In the ^{31}P-NMR spectrum of **6** below −41.5°, the coalescence temperature, two pairs of *d* resonances were observed that were assigned to the (CR^*, R^*_{axial})- and (CR^*, S^*_{axial})-diastereoisomers of **6** (*Fig. 8*). A 3.6:1 ratio of diastereoisomers, which corresponds to a $\Delta G°_{183}$ of 0.47 kcal/mol, was observed below the coalescence temperature by integration of the peak areas. The free energies of activation, ΔG^*, of the process required to render these diastereoisomers equivalent, calculated by the method of *Shanan-Atidi* and *Bar-Eli* [25] for unequal populations of exchanging species, are 10.2 and 10.8 kcal/mol. This process is reasonably assigned to the ΔG^* for inversion of the dibenzo[*d,f*][1,3,2]dioxaphosphepin ring.

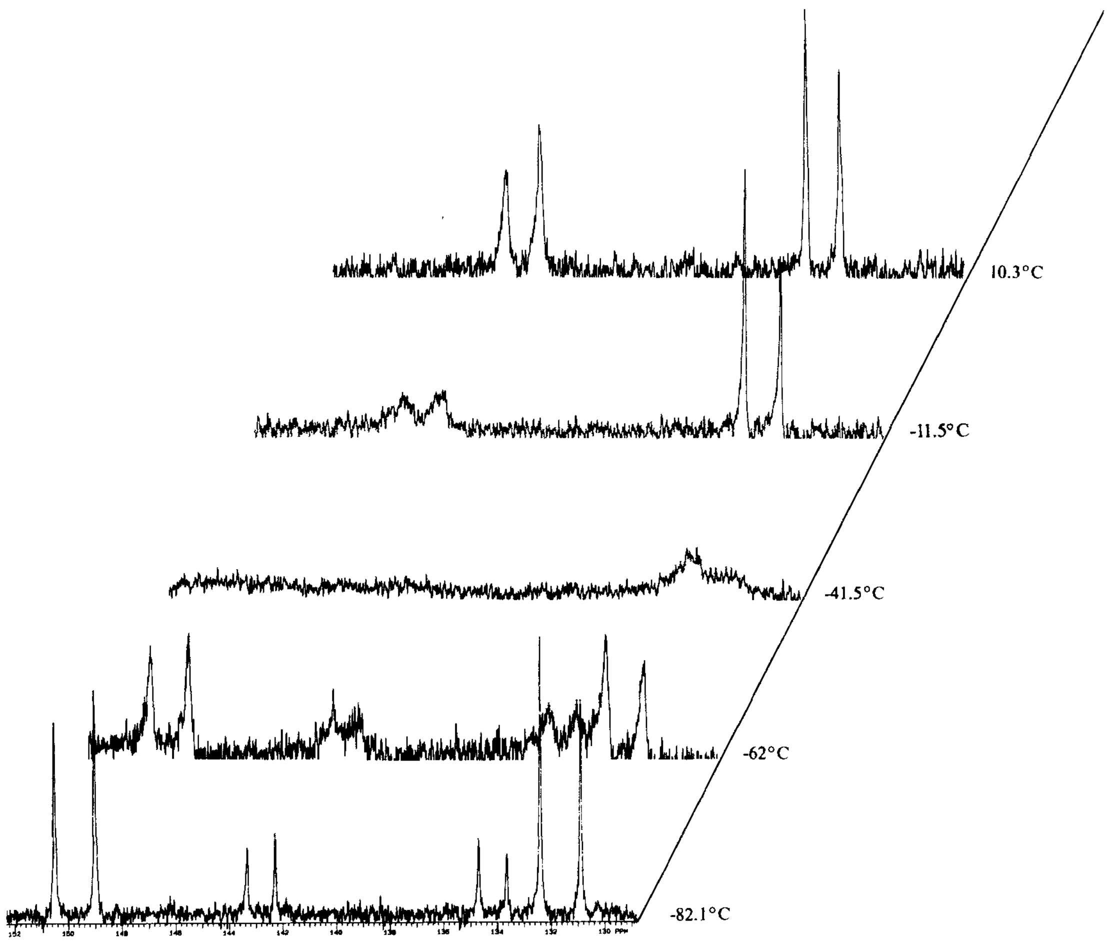

Fig. 8. *Variable-temperature ^{31}P-NMR spectra of* **6**

Quite interestingly, the $^8J(P,P)$ coupling constants observed below the coalescence temperature for the major and minor diastereoisomers of **6** were 85 and 130 Hz, respectively. The observation that the coupling constants of the individual diastereoisomers is larger than that for **6** above the coalescence temperature requires that some coupling is lost above the coalescence temperature. This must be the case, because a weighted average of the individual coupling constants for each diastereoisomer would be expected to be observed above the coalescence temperature for the rapidly interconverting diastereoisomers.

One possible explanation for the loss of P,P coupling above the coalescence temperature can be reasonably attributed to stereoelectronic or steric effects (increased P–P distance) during the ring-inversion process due to a continuous change in geometry. The transition states for ring inversion were located on the corresponding potential-energy surfaces for both **13a** and **13b** by semi-empirical MO calculations. The calculated energy barriers were 4.4 and 7.5 kcal/mol, respectively. For both **13a** and **13b**, the pathway for ring inversion involved transition states with the two aryl rings and O-atoms in a common plane with the P-atom lying above this plane. A similar transition-state geometry for the ring inversion of **6** would reasonably be expected to alter the preferred stereoelectronic arrangement for the through-space transmission of coupling information[6])[7]).

Experimental Part

General. Reagents were purchased from commercial laboratory supply houses. Solvents were dried prior to use when necessary with appropriate drying agents. Tetrahydrofuran (THF) was distilled immediately prior to use from a deep-blue soln. of sodium ketyl (sodium/benzophenone). Reactions were carried out in flame-dried apparatus under N_2 or Ar. M.p.: in open capillary tubes; *Thomas-Hoover* melting point apparatus; uncorrected. NMR Spectra: *Varian-XL-200*, *-Gemini-300*, or *-Unity-500* spectrometer; ^{31}P-NMR with full proton decoupling; $\delta(^1H)$ and $\delta(^{13}C)$ in ppm rel. to tetramethylsilane where a positive sign is downfield from the standard, $\delta(^{31}P)$ in ppm rel. to 85% phosphoric acid (external) where a positive sign is downfield from the standard, J in Hz; ^{13}C assignments from APT experiment; variable-temperature ^{31}P-NMR on a *Varian-XL-200* spectrometer. MS: *Finnigan-8200* mass spectrometer. Elemental analyes were performed by the Analytical Research Services, *Ciba-Geigy Corp.*

All calculations were performed with the PM3 method [26] [27] using either the MOPAC 5.0 [28] or SPARTAN 2.0 [29] program. The SCF convergence criteria was set to $1 \cdot 10^{-7}$ kcal/mol. Geometry optimization proceeded until the rms gradient was reduced to less than $1 \cdot 10^{-4}$ kcal/mol/Å. The stationary points so obtained were then characterized by frequency calculations which produced all positive eigenvalues for minima and a single negative eigenvalue for transition structures.

*6-Chloro-2,4,8,10-tetrakis(1,1-dimethylethyl)dibenzo[*d,f*][1,3,2]dioxaphosphepin* (**8**). To a soln. of **7** (20.00 g, 49 mmol) and 1-methylpyrrolidin-2-one (0.48 g, 4.8 mmol) in toluene (200 ml) was added dropwise at r.t. PCl_3 (10 g, 73 mmol). Then the mixture was heated to 95° and stirred at 95° for 17 h. A slow purge of N_2 was used to remove HCl. The mixture was filtered and the volatiles removed *in vacuo* 23.14 g (99%) of white solid. M.p.

---

[6]) A reviewer suggested that another plausible explanation for the reduction of P,P coupling above the coalescence temperature is that at higher temperatures there is a population of states with greater entropy ($-T\Delta S$) leading to an increased intramolecular P–P distance. This explanation is rendered unlikely, however, by the fact that no change in the magnitude of P,P coupling is observed in variable-temperature ^{31}P-NMR spectra (^{1}H-decoupled) between −25 and 60°.

[7]) Although the observed geometry in the crystal structure of **6** suggests that the lone pair of electrons on the O-atoms are not involved in a through-space coupling mechanism, similar arguments would apply to explanations involving either P or O intramolecular distances.

183–186°. ^{31}P-NMR (80.98 MHz, (D_6)benzene): 173.3. ^{1}H-NMR (200.1 MHz, (D_6)benzene): 1.23 (*s*, 18 H); 1.50 (*s*, 18 H); 7.34 (*d*, ^4J(H,H) = 2.3, 2 H); 7.59 (*d*, ^4J(H,H) = 2.3, 2 H). Anal. calc. for $C_{28}H_{40}ClO_2$: C 70.8, H 8.5; found: C 70.6, H 8.5.

*2-{1-{3,5-Bis(1,1-dimethylethyl)-2-{[2,4,8,10-tetrakis(1,1-dimethylethyl)dibenzo[*d,f*][1,3,2]dioxaphosphepin-6-yl]oxy}phenyl}ethyl}-4,6-bis(1,1-dimethylethyl)phenol* (**10**). To a soln. of **9** (27.6 g, 63 mmol) and Et_3N (8.8 ml, 63 mmol) in toluene (200 ml) was added dropwise at r.t. a soln. of **8** (30 g, 63 mmol) in toluene (100 ml). The mixture was stirred at r.t. for 20 min and then the $Et_3N \cdot HCl$ removed by filtration. The volatiles were removed *in vacuo*, and the residue was triturated with MeCN (200 ml): 40.9 (74%) of white solid. M.p. 273°–277°. ^{31}P-NMR (202.33 MHz, (D_6)benzene): 144.3. ^{1}H-NMR (300.08 MHz, (D_6)benzene): 1.06 (*s*, 9 H); 1.07 (*s*, 18 H); 1.22 (*s*, 9 H); 1.37 (*s*, 18 H); 1.63 (unresolved *d*, 3 H); 1.70 (*s*, 9 H); 3.66 (unresolved *q*, 1 H); 5.60 (*s*, 1 H, OH); 7.11 (br. *s*, 1 H); 7.20 (br. *s*, 1 H); 7.27 (br. *s*, 1 H); 7.33 (br. *s*, 1 H); 7.42 (*m*, 1 H); 7.54 (*m*, 3 H). Anal. calc. for $C_{58}H_{85}O_4P$: C 79.4, H 9.8; found: C 79.1, H 1.02.

*2-{1-{3,5-Bis(1,1-dimethylethyl)-2-{[2,4,8,10-tetrakis(1,1-dimethylethyl)dibenzo[*d,f*][1,3,2]dioxaphosphepin-6-yl]oxy}phenyl}ethyl}-4,6-bis(1,1-dimethylethyl)phenyl Phosphorodichloridite* (**11**). To a soln. of **10** (30 g, 34.2 mmol) and Et_3N (12 ml, 85.5 mmol) in xylene (250 ml) was added a soln. of PCl_3 (7.5 ml, 85.5 mmol) in xylene (40 ml). Then the mixture was heated at reflux for 28 h. The mixture was cooled to r.t. and the precipitate of $Et_3N \cdot HCl$ removed by filtration. The solvent was removed *in vacuo* and the residue triturated with MeCN (200 ml): 30 g (90%) of white solid that was used without further purification. ^{31}P-NMR (202.33 MHz, (D_6)benzene): 202.4 (*d*, ^8J(P,P′) = 136); 140.4 (*d*, ^8J(P,P′) = 136). MS: 976 (M^{+}).

*2-{1-{3,5-Bis(1,1-dimethylethyl)-2-{[2,4,8,10-tetrakis(1,1-dimethylethyl)dibenzo[*d,f*][1,3,2]dioxaphosphepin-6-yl]oxy}phenyl}ethyl}-4,6-bis(1,1-dimethylethyl)phenyl Diphenyl Phosphite* (**6**). To a soln. of **11** (28 g, 28.6 mmol) in toluene (300 ml) was added dropwise at r.t. a soln. of phenol (5.4 g, 57.2 mmol) and Et_3N (8 ml, 57.2 mmol) in toluene (20 ml). The mixture was stirred at r.t. for 18 h and then the precipitate of $Et_3N \cdot HCl$ removed by filtration. The volatiles were removed *in vacuo*, and the residue was triturated with MeCN (100 ml): 10.4 g (32%) of white solid. M.p. 164–167°. ^{31}P-NMR (202.33 MHz, (D_6)benzene): 131.2 (*d*, ^8J(P(1),P(2)) = 72.8); 141.8 (*d*). ^{31}P-NMR (CD_2Cl_2 −100°): major isomer: 150.3 (*d*, ^8J(P,P′) = 128.9); 131.2 (*d*); minor isomer: 143.1 (*d*, ^8J(P,P′) = 84.9); 133.8 (*d*). ^{1}H-NMR (499.84 MHz, (D_6)benzene): 1.23 (*s*, 9 H, *t*-Bu); 1.25 (*s*, 9 H, *t*-Bu); 1.29 (*s*, 9 H, *t*-Bu); 1.30 (*s*, 9 H, *t*-Bu); 1.33 (*s*, 9 H, *t*-Bu); 1.34 (*s*, 9 H, *t*-Bu); 1.35 (*s*, 9 H, *t*-Bu); 1.72 (*s*, 9 H, *t*-Bu); 1.94 (*d*, 3 H, *Me*CH); 6.02 (*dq*, ^6J(H,P) = 20.5, 1 H, MeC*H*); 6.66 (*t*, 1 H); 6.76 (*t*, 1 H); 6.78 (*t*, 2 H); 6.95 (*t*, 2 H); 7.18 (*d*, 2 H); 7.34 (*d*, 2 H); 6.86 (*s*, 1 H); 7.30 (*d*, 1 H); 7.32 (*d*, 1 H); 7.50 (complex *m*, 5 H). ^{13}C-NMR (125.70 MHz, (D_6)benzene): 21.90 (*dd*, *J*(C,P) = 5.6, *J*(C,P′) = 1.9); 31.24 (*s*, Me); 31.33 (*s*, Me); 31.54 (*s*, Me); 31.59 (*s*, Me); 31.60 (*s*, Me); 31.68 (*s*, Me); 31.82 (*s*, Me); 32.19 (*s*, Me); 34.63 (*s*, Me_3*C*); 34.64 (*s*, Me_3*C*); 34.66 (*s*, Me_3*C*); 34.72 (*s*, Me_3*C*); 35.46 (*s*, Me_3*C*); 35.59 (*s*, Me_3*C*); 35.90 (*s*, Me_3*C*); 36.09 (*s*, Me_3*C*); 38.52 (*dd*, ^4J(C,P′) = 11.4, ^4J(C,P′) = 26.9, Me*C*H); 120.87 (*d*, *J*(C,P) = 7.7); 121.31 (*d*, *J*(C,P) = 6.4); 123.43 (*s*); 123.80 (*s*); 123.86 (*s*); 124.18 (*s*); 124.32 (*s*); 124.35 (*s*); 124.61 (*s*); 124.65 (*s*); 124.75 (*s*); 126.99 (*s*); 128.29 (*s*); 129.65 (*s*); 133.80 (*d*, *J*(C,P) = 3.9); 134.00 (*d*, *J*(C,P) = 4.2); 135.12 (*s*); 138.68 (br. *s*); 140.82 (*d*, *J*(C,P) = 1.5); 140.88 (*d*, *J*(C,P) = 1.6); 141.86 (*d*, *J*(C,P) = 2.3); 142.09 (*s*); 145.36 (*d*, *J*(C,P) = 0.9); 145.92 (*d*, *J*(C,P) = 1.3); 146.18 (*d*, *J*(C,P) = 5.2); 146.58 (*s*); 146.68 (*s*); 146.73 (*s*); 147.11 (*d*, *J*(C,P) = 7.5); 147.66 (*dd*, *J*(C,P) = 4.0, *J*(C,P′) = 0.9); 152.49 (*d*, *J*(C,P) = 7.0); 152.79 (*s*). Anal. calc. for $C_{70}H_{94}O_6P_2$: C 76.9, H 8.7; found: C 76.9, H 9.0.

X-Ray Analysis. Suitable crystals were grown from MeCN. Intensity data was measured on a *Siemens R3MV* four-circle diffractometer as described in *Table 1*. Accurate cell measurements were obtained from 29 intense reflections ($I > 40000$), collected over the 2Θ range of 40–50°. There was no significant intensity variation for three standard reflections measured every 100 applied; no absorption or extinction corrections were applied. The structure was solved by direct methods using *Siemens* SHELXTL PLUS (VMS). Full-matrix least-squares refinements were carried out. One of the *t*-Bu groups was disordered and refined with fixed 50% occupancy for each rotamer. Positions of the C-atoms of one rotamer are illustrated in *Fig. 3* as C(52a), C(53a), and C(54a). Supplementary material was deposited with the *Cambridge Crystallographic Data Centre*.

We wish to thank *Ciba-Geigy Corp.* for support and permission to publish this work. The authors thank Ms. *Magdalena Brzechffa* for assistance in running the X-ray analysis, Ms. *Lilibeth Burke* and Mr. *Dario Bini* in obtaining the NMR spectra, and Ms. *Andrea Smith* in obtaining MS.

REFERENCES

[1] C. A. Tolman, *J. Am. Chem. Soc.* **1970,** *92,* 2956; S. Otsuka, T. Yoshida, M. Matsumoto, K. Nakatsu, *ibid.* **1976,** *98,* 5850; T. Yoshida, T. Yamagata, T. H. Tulip, J. A. Ibers, S. Otsuka, *ibid.* **1978,** *100,* 2063, and ref. cit. therein; F. G. N. Cloke, M. F. Lappert, G. A. Lawless, A. C. Swain, *J. Chem. Soc., Chem. Commun.* **1987,** 1667.

[2] S. D. Pastor, J. L. Hyun, P. A. Odorisio, R. K. Rodebaugh, *J. Am. Chem. Soc.* **1988,** *110,* 6547.

[3] G. Szalontai, J. Bakos, I. Tóth, B. Heil, *Magn. Reson. Chem.* **1987,** *25,* 761.

[4] S. D. Pastor, R. K. Rodebaugh, P. A. Odorisio, B. Pugin, G. Rihs, A. Togni, *Helv. Chim. Acta* **1991,** *74,* 1175.

[5] S. D. Pastor, A. Togni, *Inorg. Chim. Acta* **1989,** *159,* 3.

[6] E. Billig, A. G. Abatjoglou, D. R. Bryant, Eur. Pat. Appl. 213639 (*CA*: *107,* 7392).

[7] S. D. Pastor, A. Togni, *J. Am. Chem. Soc.* **1989,** *111,* 2333; *J. Org. Chem.* **1990,** *55,* 1649; A. Togni, S. D. Pastor, G. Rihs, *J. Organomet. Chem.* **1990,** *381,* C21; for related studies, see S. D. Pastor, *Tetrahedron* **1988,** *44,* 2883; A. Togni, S. D. Pastor, G. Rihs, *Helv. Chim. Acta* **1989,** *72,* 1471; A. Togni, S. D. Pastor, *Tetrahedron Lett.* **1989,** *30,* 1071; *ibid.* **1990,** *31,* 839; A. Togni, R. Häusel, *Synlett* **1990,** 633; A. Togni, S. D. Pastor, *Chirality* **1991,** *3,* 331; S. D. Pastor, R. Kesselring, A. Togni, *J. Organomet. Chem.* **1992,** *429,* 415.

[8] K. Kushioka, *J. Org. Chem.* **1983,** *48,* 4948.

[9] M. M. Crutchfield, C. H. Dungan, J. H. Letcher, V. Mark, J. R. Van Wazer, 'Topics in Phosphorus Chemistry', Eds. M. Grayson and E. J. Griffith, Wiley, New York, 1967, Vol. 5; J. G. Verkade, L. D. Quin, 'Phosphorus-31 NMR Spectroscopy in Stereochemical Analysis', VCH, Weinheim, 1987; 'Handbook of Phosphorus-31 Nuclear Magnetic Resonance Data', Ed. J. C. Tebby, CRC, Boca Raton, 1991.

[10] P. A. Odorisio, S. D. Pastor, J. D. Spivack, D. Bini, R. K. Rodebaugh, *Phosphorus Sulfur* **1984,** *19,* 285.

[11] P. A. Odorisio, S. D. Pastor, J. D. Spivack, *Phosphorus Sulfur* **1984,** *19,* 1.

[12] W. M. Abdou, D. B. Denney, D. Z. Denney, S. D. Pastor, *Phosphorus Sulfur* **1985,** *22,* 99.

[13] a) L. Petrakis, C. H. Sederholm, *J. Chem. Phys.* **1961,** *35,* 1243; b) S. Ng, C. H. Sederholm, *ibid.* **1964,** *40,* 2090; c) J. Hilton, L. H. Sutcliffe, *Progr. NMR Spectrosc.* **1975,** *10,* 27; d) J. D. Goddard, A. W. Payne, N. Cook, H. R. Luss, *J. Heterocycl. Chem.* **1988,** *25,* 575; e) F. B. Mallory, C. W. Mallory, M. B. Baker, *J. Am. Chem. Soc.* **1990,** *112,* 2577; f) L. Ernst, *J. Chem. Soc., Chem. Commun.* **1977,** 375; g) R. A. Pascal, Jr., A. P. West, Jr., D. Van Engen, *J. Am. Chem. Soc.* **1990,** *112,* 6406.

[14] J. J. P. Stewart, *J. Comput.-Aided Mol. Design* **1990,** *4,* 1.

[15] A. Mannschreck, L. Ernst, *Chem. Ber.* **1971,** *104,* 228.

[16] A. Mannschreck, L. Ernst, E. Keck, *Angew. Chem. Int. Ed.* **1970,** *9,* 806.

[17] N. L. Allinger, M. T. Tribble, *Tetrahedron Lett.* **1971,** 3259.

[18] S. D. Pastor, J. D. Spivack, L. P. Steinhuebel, C. Matzura, *Phosphorus Sulfur* **1983,** *15,* 253.

[19] B. A. Arbusov, R. A. Kadyrov, R. P. Arshinova, N. A. Mukmeneva, *Izv. Akad. Nauk SSSR* **1981,** 784.

[20] For a review, see L. D. Quin, in 'Conformational Analysis of Medium-Sized Heterocycles', Ed. R. S. Glass, VCH, Weinheim, 1988, pp. 193–194.

[21] J. Hans, R. O. Day, L. Howe, R. R. Holmes, *Inorg. Chem.* **1992,** *31,* 1279; T. K. Prakasha, R. O. Day, R. R. Holmes, *ibid.* **1992,** *31,* 1913.

[22] K. C. Kumara Swamy, R. O. Day, J. M. Holmes, R. R. Holmes, *J. Am. Chem. Soc.* **1990,** *112,* 6095; S. D. Burton, K. C. Kumara Swamy, J. M. Holmes, R. O. Day, R. R. Holmes, *ibid.* **1990,** *112,* 6104; T. K. Prakasha, R. O. Day, R. R. Holmes, *Inorg. Chem.* **1992,** *31,* 725.

[23] M. J. Baker, K. N. Harrison, A. G. Orpen, P. G. Orpen, P. G. Pringle, G. Shaw, *J. Chem. Soc., Chem. Commun.* **1991,** 803.

[24] M. Nógrádi, 'Stereochemistry: Basic Concepts and Applications', Pergamon, Oxford, 1981, pp. 112–126; E. Juaristi, 'Stereochemistry and Conformational Analysis', Wiley, New York, 1991, pp. 91–105.

[25] H. Shanan-Atidi, K. H. Bar-Eli, *J. Phys. Chem.* **1970,** *74,* 961.

[26] J. J. P. Stewart, *J. Comput. Chem.* **1989,** *10,* 209.

[27] J. J. P. Stewart, *J. Comput. Chem.* **1989,** *10,* 221.

[28] 'QCPE 455, MOPAC 5.0', Department of Chemistry, University of Indiana, Bloomington, IN 47405.

[29] 'SPARTAN 2.0', *Wavefunction, Inc.*, Irvine, CA 92715.